

# Failure Characteristics of Roof Falls at an Underground Stone Mine in Southwestern Pennsylvania

**Anthony T. Iannachione**, Deputy Director  
**Thomas E. Marshall**, Engineering Technician  
**Leonard J. Prosser**, Research Physical Scientist  
NIOSH - Pittsburgh Research Laboratory  
Pittsburgh, PA

## ABSTRACT

The location and time of 2,007 microseismic emissions from a limestone mine in southwestern Pennsylvania were compared with the development of mine faces and the characteristics of the mine layout. Based on analyses of these results, the occurrence of roof failure zones appears to be associated with certain characteristics of the mine plan. It was determined that significant relationships exist between the intensity of the microseismic activity and the scale of the roof failures. Microseismic activity associated with these roof falls occurs in distinct episodes, with the final failure event occurring during approximately a 12-hour period. Each roof fall episode appears to be composed of dozens of distinct roof beam failures. As each beam fails in shear and tension, tens to hundreds of audible noises representing rock fracturing or bedding plane separation can occur. While every roof fall can be viewed as unique, certain mechanistic similarities can be realized through careful observation and monitoring of these complex systems. Understanding these similarities in characteristics allows mine personnel to design the most effective and efficient control technique.

## INTRODUCTION

Falls of roof and rib in underground mines are, at best, difficult to anticipate. Miners are far too often injured by unexpected falls-of-ground. Mitigation of this type of accident is highly dependent upon a sound understanding of the interaction of the local geology, stress field, mining practices, and mine layout. One significant gap is how excessive levels of stress redistribute in response to mining and how these stresses affect rock failure. To address this knowledge gap, a comprehensive field investigation was undertaken to characterize important features of rock failure in an underground limestone mine in southwestern Pennsylvania using both observational and microseismic monitoring data from February 9, 2000, until November 17, 2000. Information on the extent and occurrence of roof failures and the location and timing of microseismic activity were examined and compared with changes to mine layout.

### Field Site Conditions

The study underground mine produces crushed stone at overburdens ranging from 60 to 120 m (200 to 400 ft). Within the

study section of the mine, two different room-and-pillar mine layouts were used. Throughout most of the study area, a traditional room-and-pillar layout was used where rooms 13.8 m (45 ft) wide by 7.6 m high (25 ft) were driven N 10° E and N 80° W on 24.4 m (80 ft) centers outlining 10.7 m (35 ft) square pillars. In the northeastern section of the study area, a new stress-control room-and-pillar layout was tried. Room sizes were not changed from the old design; however, pillar sizes and mining orientations were modified. In the northeastern section, rectangular pillars measuring 27.4 by 15.2 m (90 by 50 ft) were mined with the long axis oriented approximately N 55° E. In all areas of the operation, the limestone was mined by blasting V-cuts 4 m (13 ft) deep in various entries along a wide mining front. Additionally, some bench cuts 10.7 m (35 ft) deep were made in the central portion of the mine. Figure 1 shows the location of all development and bench production cuts made in this section during the study period.

At the study mine, the crushed stone is produced from the Loyalhanna Limestone Formation, which averages 21.5 m (70 ft) thick in this area. It is overlain by the Mauch Chunk Formation, containing interbedded shales and calcareous sandstones, and underlain by the Pocono Sandstone. While the strengths of intact specimens are very high (UCS 130 to 200 MPa), the Loyalhanna Limestone contains numerous structures that significantly influence the overall rock mass strength. The largest scale features are reverse or thrust faults with as much as several meters of displacement. Large trough beds, which can extend from several meters to tens of meters in length, dip at angles ranging from 70 to 20 degrees. Jointing is generally widely spaced but often extends through the entire mining horizon. Bedding planes extend over large areas of the mine and are often used to form smooth roof horizons in the mine. These planes are close to horizontal and are spaced at intervals ranging from several centimeters to several meters. The smallest scale structures are crossbeds that dip from 15 to 35 degrees and are spaced at intervals averaging one centimeter. These structures can have considerable influence on the size, shape, scale, and pattern of roof rock failures observed in the study area.

### Roof Rock Failures

Roof falls found at this mine fit the characteristics of those caused by excessive levels of horizontal stress (5 and 6). Roof instabilities typically begin with the development of compression zones consisting of low-angle shears oriented approximately N 30°

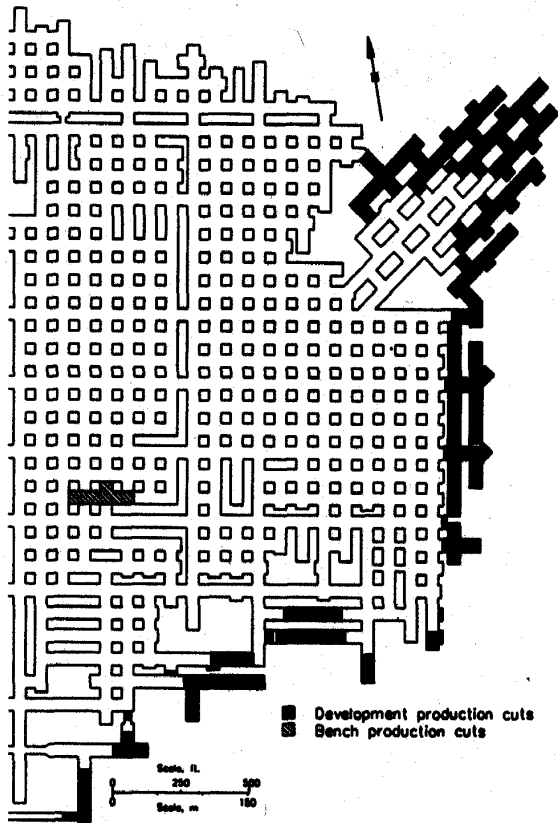


Figure 1 - Mine layout showing the location of production cuts mined during the study period.

W. When roof falls occur, many of them are oval in shape with the long axis oriented approximately N 30° W. In the northeastern section of the mine, these roof falls follow this same northwesterly direction (Figure 2). All of these failure patterns support the existence of a pervasive horizontal stress field oriented approximately N 60° E. Hydrofracturing tests at this mine site measured the maximum stress direction between N 60° and 75° E (3). Additionally, measurements of the horizontal stresses in the limestone roof rock are very high, ranging from 15 to 55 MPa (2,200 to 8,000 psi).

During the study period, four distinct roof falls, one roof fall extension, several cutter roof failures, and numerous roof skin failures occurred (Figure 2). The four roof falls occurred in the southeastern corner of the mine, an area where excessive levels of horizontal stress were concentrated as the mine continued to develop into the NE-SW oriented stress field (4).

The four roof falls were characterized as such because these roof failures propagated above the 2.4 m (8 ft) roof bolted interval. Each of the four roof falls had similarities, yet also had distinct forms and occurrence. Similarities include: 1) failure through approximately 3 m (10 ft) of limestone roof, 2) failure into an exceedingly weak clayey shale member above the top of the limestone roof member, and 3) failures occurred through limestone

roof consisting of numerous distinct roof beams of varying strength. Distinct features include: 1) failures developed over both extensive time periods measured in months and relatively short time periods of intense activity measured in hours, and 2) failure zones were often intercepted by large-scale geologic structures.

Smaller-scale roof failures, including cutter roof and roof skin damage, occurred near the four roof falls, along the eastern mining front, along a N 30° W trend extending through the southern portion of the study area, and along another N 30° W trend extending through the northern portion of the study area (Figure 2). Small-scale roof failures are defined as those which do not propagate above the 2.4 m (8 ft) roof bolted horizon. The cutter roof failures occur when a highly stressed roof beam shears or cuts perpendicular to the principal direction of the applied force. These shears occur at a low-angle, approximately 15°, and propagate laterally at a rate that can be measured in meters per minute to meters per hour. Within the study area, the cutter roof failures were generally oriented N 30° W. Roof skin damage occurs when the very lowest layers of the roof beam fail over a considerable portion of the mine room. These failures generally occur within days or weeks after mining and produce a very rough or wavy roof.

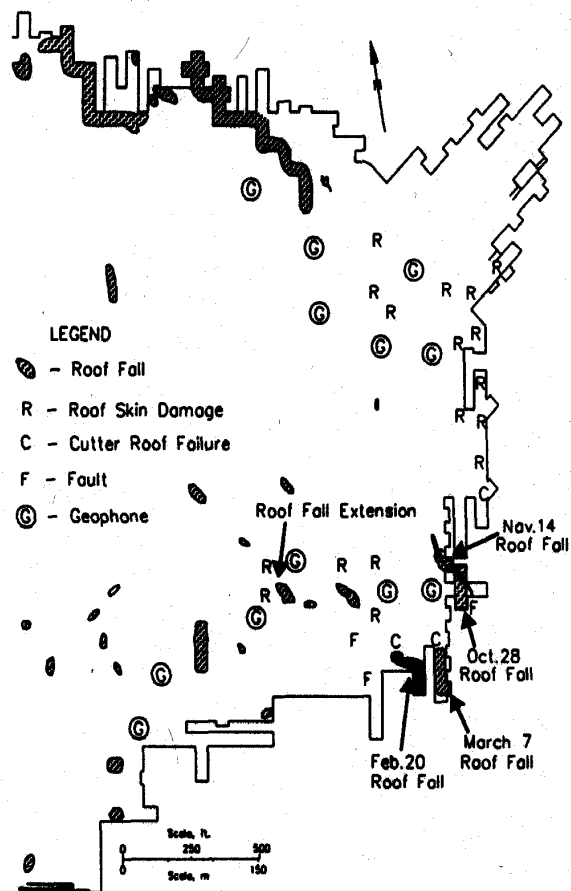


Figure 2 - Location of roof falls, roof skin damage, cutter roof failure, faults, and geophones present at the end of the study.

## MICROSEISMIC ACTIVITY

Microseismic monitoring began on February 9, 2000, and information reported on in this study extends from this date until November 17, 2000. The monitoring system consisted of 12 geophones located throughout the study area (Figure 2), data acquisition, filtering, and analysis equipment located in a trailer, and cables connecting the geophones to the instrument trailer. The maximum distance across the geophone array was 550 m (1,800 ft). The dominant frequency response for this system is between 0.1 and 250 Hz.

It is widely known that as rock fails it emits audible sounds. Hardy (2) examined this concept when he stated: "In geologic materials the origin of acoustic emissions/microseismic activity is not well understood, but it appears to be related to processes of deformation and failure which are accompanied by a sudden release of strain energy." Microseismic monitoring systems can be designed and placed in such a way so as to locate the source of energy release associated with roof failure. With this tool, the relative quantity of roof damage can be monitored continuously as mining progresses.

During this study, 2,007 microseismic events attributable to rock failure were analyzed. The distribution of these events is shown in Figure 3. The majority of the activity occurred along the southeastern mining front where a traditional room-and-pillar layout was used. In contrast, the northeastern mining front, using the stress-control layout, had much less activity. In a previous study, the authors determined that the stress control layout was superior to the traditional room-and-pillar layout in controlling damaging horizontal stress concentrations, hence, lessening the occurrence of rock failure and associated microseismicity (4).

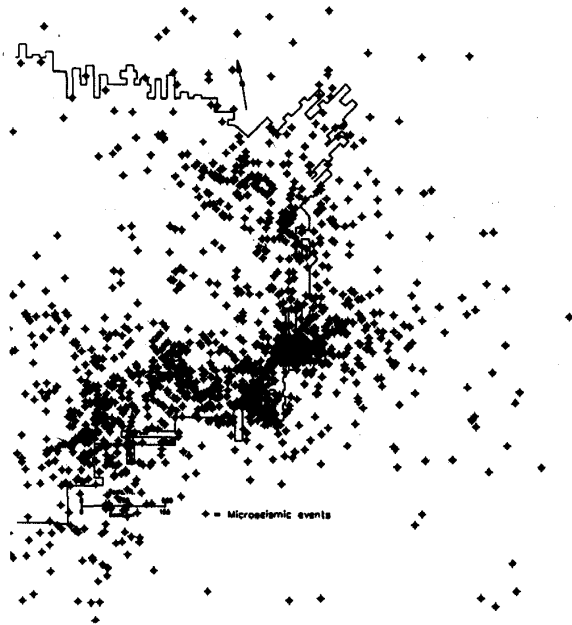


Figure 3 - Location of microseismic events.

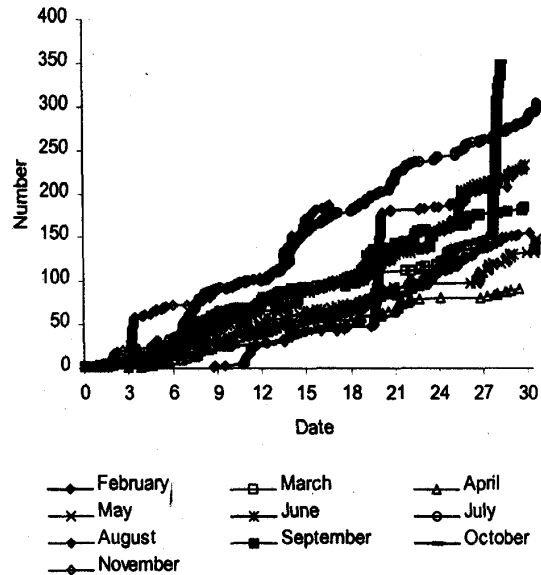


Figure 4 - Microseismic activity by month.

It is evident from Figure 3 that some of the activity during certain months is concentrated in distinct zones. It should be noted that the most dense areas of activity appears in the southeast corner of the study area, where the four roof falls occurred. Intervals of increased activity can be determined when the events are plotted against time for each of the months (Figure 4). In general, the average rate of background microseismic activity for this study ranged between 0.14 and 0.35 events/hour. The background average activity rate was highest in November and lowest in April.

Of particular interest to this study are the time periods when significant rate increases occur in microseismic activity. Six-hundred-thirteen events, or 31% of the total number of events, occurred during these periods of elevated microseismic activity. These periods had rates ranging from 0.5 to 12.3 events/hour (Table 1). The number of events measured during these periods of increased activity ranged from 14 to 204, and the durations of this increased activity ranged from 5 to 40 hours.

Three general categories of elevated microseismic activity were identified and classified as activity associated with massive, moderate, and slight roof failures. For example, in the massive roof failure category, two roof falls (Feb. 20 and Oct. 28) produced the most events and the highest event rates. In contrast, two other roof falls (March 7 and Nov. 14) were much lower in the number and rate of events in comparison to other episodes of elevated microseismic activity. Explanations for these differences are provided later. In the moderate roof failure category, only the June 26 roof fall extension was identified, producing 37 events over a 5-hour period. Several slight roof failures were observed with event rates ranging from 0.5 to 2.3 events/hour. This category of elevated microseismic activity was associated with the occurrence of cutter roof and roof skin failures or, in some situations, no observable roof damage (Table 1).

Start date	Duration, hr	# of events	Rate, events/hr	Remarks	Spatial event clustering
11-Feb	9.54	20	2.1	No Observable Roof Damage	Slight
20-Feb	13.96	130	9.3	Roof Fall	Dense
7-Mar	11.16	23	2.1	Roof Fall	Slight
21-Apr	27.44	14	0.5	No Observable Roof Damage	None
27-May	19.65	21	1.1	Shallow Roof Failure	Moderate
24-Jun	10.09	23	2.3	No Observable Roof Damage	None
26-Jun	4.99	37	7.4	Prior Roof Fall Extension	Moderate
7-Jul	39.54	51	1.3	Some Small Roof Damage	Moderate
14-Jul	14.09	28	2.0	No Observable Roof Damage	None
20-Sep	12.68	29	2.3	Some Small Roof Damage	Slight
28-Oct	16.58	204	12.3	Roof Fall	Dense
14-Nov	6.39	33	5.2	Roof Fall	Slight

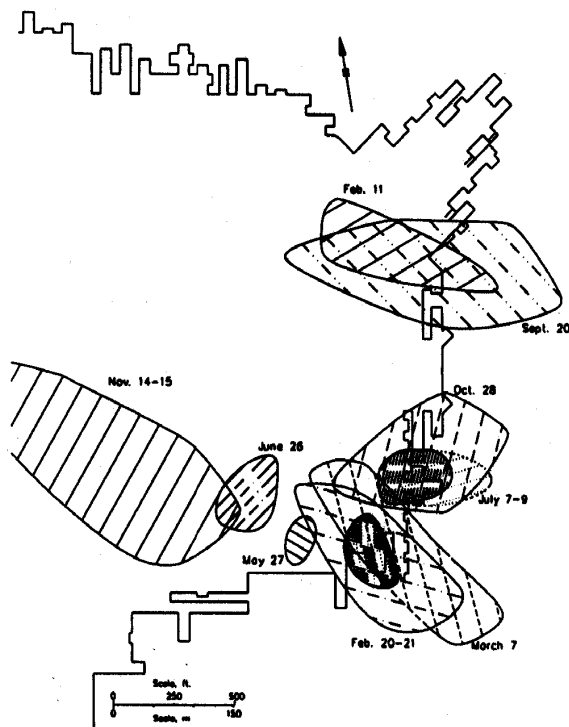


**Figure 5 - Zones of elevated microseismic activity.** The density of the hatch pattern provides a relative indicator of the density of microseismic events.

Plots of the microseismic activity associated with each of the dates listed were analyzed. When the events concentrated within a definable zone that was considered significant, that zone was mapped and placed on Figure 5. Of the 12 dates listed in Table 1, nine had enough clustering to plot a zone of intensity. The three dates with event locations that were too scattered to plot a zone of intensity were April 21, June 24, and July 14. On all three of these days, no significant roof failures were observed in the study area. Therefore, the cause of the elevated microseismic activity during these dates is unknown and may not be directly related to a localized, well-defined, rock failure episode.

Some observations based on the plots displayed in Figure 5 can be made.

- The size of the activity intensity zone is related to the density or clustering of events within that zone. The zones that are most dense appear to be smallest in area while zones that are least dense appear to have the largest areas. For example, the densest activity zones were associated with the Feb. 20 and Oct. 28 roof falls, where the strength of the microseismic events was observed to be high. Here the strong events were located with a greater degree of accuracy by the location algorithm.
- All of the activity intensity zones overlap in four distinct areas of the mine. During the study period, these zones were areas where roof failure was observed underground (Figure 2).
- In several cases, the general shape of the activity intensity zones is elliptical, with the long axis oriented approximately NW-SE. Since the principal orientation of the horizontal stress field is approximately  $N 60^{\circ} E$ , failures related to this stress field should be oriented  $N 30^{\circ} W$ .
- While the duration of individual roof rock failure episodes in the study area ranged from 5 to 40 hours, many of these areas were subjected to repeated roof rock failure episodes.

It should be noted here that factors different from those identified above may be responsible for the character of the microseismic activity. For example, the elliptical shape of the zones of elevated microseismic activity could be related to the elliptical shape of the seismic array. With such an array, the orientation of many event location error ellipsoids could be NW-SE. The role played by array geometry in defining the shape of these distributions has not been ascertained.

Another possible factor that could be considered if sufficient data existed is geology. Large, unobserved geologic structures, such as faults, may exist adjacent to the underground mine, controlling the distribution and shape of microseismic activity. Additionally, the geologic character of the roof rock has not been mapped and, therefore, may be a controlling factor in determining roof rock stability. For example, a significant number of the roof failures may occur in a particular arrangement of geologic structures or within a particular geologic horizon. Unfortunately, observations of roof geology are, at best, marginally in roof fall areas, and, at worst, nonexistent in good roof areas. Therefore it is not practical to collect this type of information in the level of detail needed, making it difficult to consider their impact.

## CHARACTERISTICS OF ROOF ROCK FAILURE EPISODES

One of this study's aims was to identify specific characteristics of significant roof failure episodes. To this end, the detailed characteristics of the four roof falls are presented so that possible roof failure mechanisms can be discussed.

### The February 20 and March 7 Roof Falls

On February 20, 2000, a roof fall occurred in the southeast corner of the mine (Figure 2). In this area, a prominent low angle shear, or cutter roof failure had first formed in August of 1999. Since microseismic monitoring did not begin until 11 days before the roof fall, it was not possible to determine what activity occurred over the 6 month period between the first failure and the February 20 roof fall. On February 20 intense microseismic activity began around 2:30 pm and continued for approximately 14 hours (Figure 6). During this time 130 events, occurring at an average rate of 9.3 events/hour, were recorded within and adjacent to the roof fall. Because this roof fall occurred on a Sunday, no mine personnel were in the mine to witness it. However, there was still some audible activity connected with the roof fall on Monday February 21. At approximately 4:00 pm activity quieted considerably and no additional failures were observed.

Over the next 12 days the activity level in this area was relatively low. On March 7, there was a sudden increase in activity with 23 events occurring over approximately 11 hours for a rate of 2.1 events/hour before leveling off to more typical background rates (Figure 7). During this time mine personnel reported loud, audible noises from the rock and observed episodes of roof failure. Of interest to this study is the fact that the February 20 roof fall extended approximately 68 m (220 ft) in length while the March 7 roof falls extended approximately 45 m

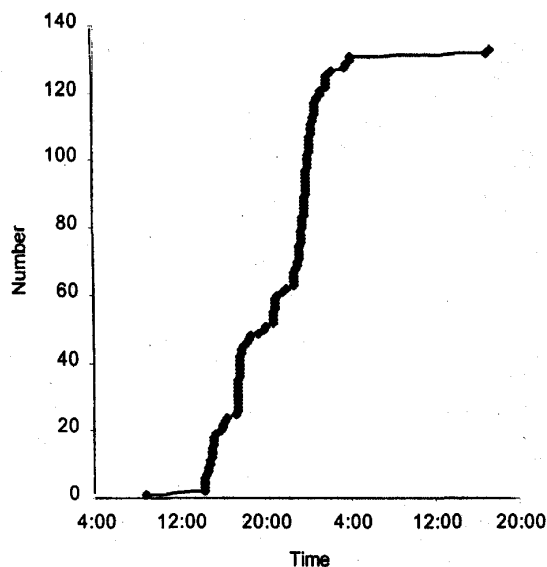


Figure 6 - Microseismic activity during the February 20-21, 2000 roof fall.

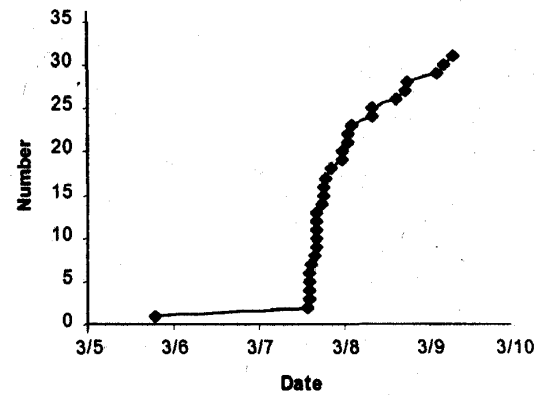


Figure 7 - Microseismic activity during the March 7, 2000 roof fall.

(150 ft). This may partially explain the difference in activity intensity during the March 7 roof fall. Additionally these roof falls were separated by only 10.7 m (35 ft) of barrier pillar. Therefore some of the roof over the March 7 roof fall may have failed during the very active February 20 roof fall. It is also important to note that both roof falls were preceded by a period of extreme quiet and that both falls were approximately 1/2 day in duration.

### The October 28 and November 14 Roof Falls

On October 28, 2000, a roof fall occurred in the southeast corner of the mine (Figure 2). In this area, a prominent low-angle shear (cutter roof failure) had first formed sometime after the March 7 roof fall. The area remained relatively inactive until July 7 (Figure 5). At this time, shearing occurred in the immediate roof, causing a shallow roof fall to extend over a relatively large area. Again, a period of relative inactivity occurred until early on October 28, when approximately 50 microseismic events were recorded over a two-hour period (Figure 8). It is assumed that numerous thin beds within the immediate roof failed along bedding and through the intact material. This period was followed by another period of relative quiet lasting approximately three hours. Then almost 50 events were recorded over a 20 minute period. Again, a period of relative quiet occurred for approximately 2 hours. Next, a third period of high activity occurred over the next hour, followed by approximately 8 hours of relatively small events at fairly constant rates. It is possible that during this time period both the edges and top of the roof fall continued to increase in size. This roof fall occurred on a Saturday and was not discovered by mine personnel until November 1. The activity associated with this roof fall lasted approximately 16 hours and included 204 events, giving a rate of 12.3 events/hour.

Over the next 16 days, the activity level in this area was relatively low. On November 14, there was a sudden increase in activity, with 33 events occurring over approximately 6.4 hours for a rate of 5.2 events/hour before leveling off to more typical background rates. During this time, mine personnel were in the section to observe or hear episodes of roof failure. As with the February 20 roof falls, the October 28 roof fall was somewhat

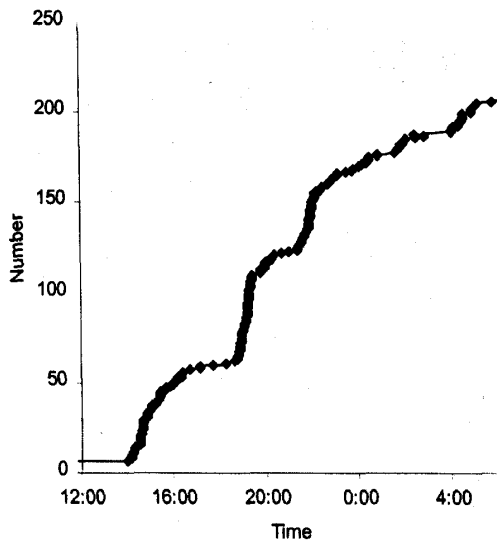


Figure 8 - Microseismic activity associated with the October 28, 2000 roof fall.

larger, extending approximately 55 m (180 ft) in length while the November 14 roof falls extended approximately 26 m (85 ft) in length. Here again, the second and smaller roof fall produced significantly less activity. Additionally, these roof falls were separated by only a portion of the 10.7-m (35-ft) barrier pillar. It is again assumed that some of the roof over the November 14 roof fall may have failed during the very active October 28 roof fall. It is also important to note that both roof falls were preceded by a period of quiet and that the duration of intense activity for both falls ranged from 7 to 16 hours.

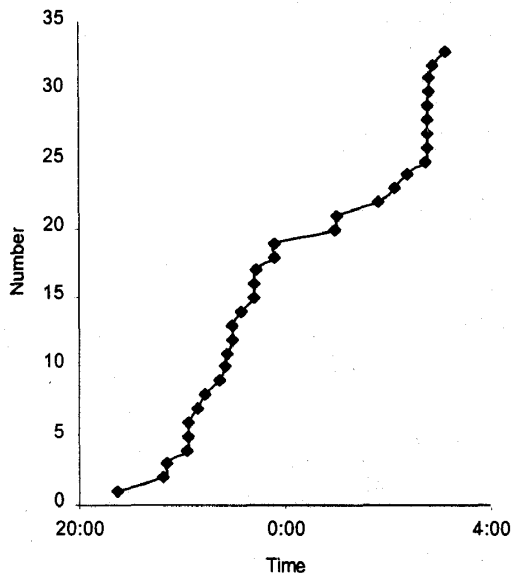


Figure 9 - Microseismic activity associated with the November 14, 2000 roof fall.

What is most interesting about these data is that most of the November 14 events did not plot over the roof fall area, but were instead located hundreds of meters away towards the center of the mine (Figure 5). Much of this activity is located adjacent to an active bench area. The slender bench pillars could have allowed the overlying limestone roof layers to deflect slightly and separate from the overlying Mauch Chunk Formation. However, it does not seem likely that the distant November 14 events could have produced enough dynamic shaking to cause the November 14 roof fall. Additional information will be needed to understand the relationship between the November 14 roof fall, the remote distribution of events, and any possible deformation mechanisms that might link the two.

#### Apparent Mechanism for Roof Rock Failure

Typically, roof failure starts when one of the stiffest and/or thinnest beds in the roof strata concentrates enough horizontal compressional stresses to initiate both intact shear failure and adjacent tensile bedding plane failures. Gale et al.(1) proposed this mechanism for roof failure, identifying five possible in situ rock failure modes. These failures would damage the roof rock skin and might produce the distinctive cutter roof failure. Through time, stresses in the intact roof beams above the initial failed beams remain high. At this point, low-angle shears and the accompanying vertical tensile failures could occur suddenly in the remaining intact isolated roof beams, whose vertical confinement would have been reduced. As various roof beams fail, stresses are transferred to adjacent beams where the process is repeated.

Because the roof failures extended from 6 to 10 m (20 to 30 ft) into the roof and from 26 to 68 m (85 to 220 ft) in length, a single roof fall could easily involve hundreds to thousands of individual shear failures (microseismic events). It appears that this process takes hours to complete and the activity only subsides when the roof fall cavity begins to assume a more stable arch shape.

#### SUMMARY AND CONCLUSIONS

A summary of information contained within this report follows:

- The roof rock in the study area was composed of 3 to 4.6 m (10 to 15 ft) of limestone with individual beams of varying thickness and strength.
- Both roof falls and regions of roof damage were generally oriented N 30° W. This suggests that a strong N 60° E horizontal stress field exists throughout the study area. In situ stress measurements and stress mapping verify this observation.
- Microseismic activity included 1,394 background events occurring at a rate ranging from 0.14 to 0.35 events/hour. Additionally, 613 events were associated with one of twelve periods of elevated microseismic activity. The activity rate during these periods ranged from 0.5 to 12.3 events/hour.
- Nine of the twelve periods of elevated microseismic activity produced event clusters dense enough to contour. With one exception, these contoured areas were associated with observable roof failures. The failures ranged from the simple formation of cutter roof failure and/or the development of roof skin damage to large roof falls. Half of the event clusters were elliptical in shape, with the long axis of the ellipse parallel with

the orientation for rock failures of this mine and perpendicular to the measured maximum horizontal stress direction. All periods of elevated microseismic activity were preceded by periods of very low activity.

- The size of the zone of elevated microseismic activity is related to the density or clustering of events within that zone. All of the zones overlap in four distinct areas of the mine.
- While the duration of individual roof rock failures episodes in the study area ranged from 5 to 40 hours, many of these areas were subjected to repeated roof rock failure episodes.
- The February 20 and October 28 roof falls were similar in that considerable time elapsed (6 to 7 months) between the occurrence of the first rock failures as detected by observations and microseismic activity and the final roof fall collapse. During the final failure episode, hundreds of events were recorded over a 9- to 16-hour period.
- The March 7 and November 14 roof falls were similar in that they occurred adjacent to (10 m away) and shortly after (12 to 16 days) the previous roof falls. During these secondary failure episodes, event totals were much lower (20 to 30 events), which could indicate collateral damage from the adjacent roof fall episodes.

In conclusion, the occurrence and location of roof failure zones appears to be associated with certain interactions between the local geology, stress field, mining practices, and mine layout. Significant relationships exist between the intensity of the microseismic activity and the scale of the roof failures. Microseismic activity associated with roof falls occurs in distinct episodes with the final failure event occurring during approximately a 12-hour period. Each roof fall episode is probably composed of many distinct roof beam failures. As each beam fails in shear and tension, tens to hundreds of audible noises representing rock fracturing or bedding plane separation can occur. Each roof rock failure is unique because of the distinctive character of local geology, stress, and mine layout. However, certain mechanistic similarities can be realized through careful observation and monitoring of these complex systems. Understanding the unique failure path that different rocks follow allows mine personnel to implement the most effective and efficient administrative or engineering control technique.

#### REFERENCES

1. Gale, W.J., Heasley, K.A., Iannacchione, A.T., Swanson, P.L., Hatherly, P., and King A., "Rock Damage Characterisation from Microseismic Monitoring," Proceedings of the 38<sup>th</sup> U.S. Rock Mechanics Symposium, Washington, D.C., July 7-10, 2001, in press.
2. Hardy, R., "Emergence of AE/MA as a Tool in Geomechanics," First Conference on Acoustic Emission-Microseismic Activity in Geologic Structures and Materials, University Park, PA, June 9-11, 1975, Series on Rock and Soil Mechanics, Vol. 2, No.3, by Trans Tech Publications, Rockport, MA, pp.13-31.
3. Iannacchione, A. T., D. R. Dolinar, L. J. Prosser, T. E. Marshall, D. C. Oyler, and C. S. Compton, "Controlling Roof Beam Failures from High Horizontal Stresses in Underground Stone Mines," Proceedings of the 17<sup>th</sup> International Conference on Ground Control in Mining, Morgantown, WV, Aug.4-6, 1998, pp.102-112.
4. Iannacchione, A., Marshal, T.E., Burke, L., Melville R. & Litsenberger J.E., "Safer Mine Layouts for Underground Stone Mines Ssubjected to Excessive Levels of Horizontal Stress," Society of Mining Engineer's Annual Meeting, Preprint 01-88 Denver CO. Feb 26-28, 2001, 7 pp.
5. Parker, J., "Mining in a Lateral Stress Field at White Pine," Canadian Institute of Mining and Metallurgy Transactions, Vol. LXIX, 1966, pp. 375-383.
6. Mucho, T.P. and Mark, C., 1994, "Determining Horizontal Stress Direction Using the Stress Mapping Technique," 13th Conference on Ground Control in Mining, Morgantown, WV, pp. 277-289.